Inorg. Chem. **2006**, *45*, 9780–9788

Inorganic Chemistry

Article

Rational Design of 0D, 1D, and 3D Open Frameworks Based on Tetranuclear Lanthanide(III) Sulfonate–Phosphonate Clusters

Zi-Yi Du, Hai-Bing Xu, and Jiang-Gao Mao*

State Key Laboratory of Structural Chemistry, Fujian Institute of Research on the Structure of Matter, Chinese Academy of Sciences, Fuzhou 350002, People's Republic of China

Received July 17, 2006

Hydrothermal reactions of lanthanide(III) salts with *m*-sulfophenylphosphonic acid (H_3L^1) and 1,10-phenanthroline (phen) or *N*,*N*′-piperazinebis(methylenephosphonic acid) (H_4L^2) afforded six novel lanthanide(III) sulfonate–phosphonates based on tetranuclear clusters, namely, $[La_2(L^1)_2(phen)_4(H_2O)]\cdot 4.5H_2O$ (**1**), $[Ln_2(L^1)_2(phen)_2(H_2O)_5]\cdot 3H_2O$ (Ln = Nd, **2**; Eu, **3**; Er, **4**), and $[Ln_2(HL^1)(H_2L^2)_2(H_2O)_4]\cdot 8H_2O$ (Ln = La, **5**; Nd, **6**). Compounds **2**–**4** contain discrete tetranuclear lanthanide(III) cluster units in which four lanthanide(III) ions are bridged by two tridentate and two tetradentate phosphonate groups. In compound **1**, the tetranuclear clusters are further interconnected into a 1D chain through the coordination of the sulfonate groups. The structures of compounds **5** and **6** can be viewed as a 3D architecture based on a different types of tetranuclear cluster units that are interconnected by bridging H_2L^2 anions. In the tetranuclear clusters of compounds **5** and **6**, the four lanthanide(III) centers are interconnected by only two HL^1 ligands. Compound **2** is a luminescent material in the near-IR region, whereas compound **3** displays a strong luminescent emission band in the red-light region. Magnetic property measurements of compounds **2**–**4** and **6** indicate that there are strong antiferromagetic interactions between magnetic centers within the cluster units.

Introduction

The chemistry of metal phosphonates has been a research field of rapid expansion in recent years, which is mainly due to their potential application in the area of catalysis, ion exchange, proton conductivity, intercalation chemistry, photochemistry, and material chemistry.[1] Compared with the intensively studied phosphonates of the d-block transition metals as well as some main-group metals, reports on lanthanide phosphonates are still limited and a number of them are based on powder X-ray diffraction (XRD).[2−13] There are two main obstacles for the structural studies on lanthanide phosphonates: low solubility and poor crystallinity. Lanthanide compounds may exhibit useful luminescent properties in both visible and near-IR regions; hence, the elucidation of the structures of lanthanide phosphonates is very important.[14] To improve the solubility and crystallinity of lanthanide phosphonates, additional functional groups such as crown ether, carboxylate, hydroxyl, and amine groups have

---

* To whom correspondence should be addressed. E-mail: mjg@ms.fjirsm.ac.cn.

(1) (a) Clearfield, A. Metal phosphonate chemistry. In *Progress in Inorganic Chemistry*; Karlin, K. D., Ed.; John Wiley & Sons: New York, 1998; Vol. 47, pp 371−510 (and references cited therein). (b) Maeda, K. *Microporous Mesoporous Mater.* **2004**, *73*, 47 (and references cited therein).

(2) (a) Serpaggi, F.; Férey, G. *J. Mater. Chem.* **1998**, *8*, 2749. (b) Cao, G.; Lynch, V. M.; Swinnea, J. S.; Mallouk, T. E. *Inorg. Chem.* **1990**, *29*, 2112. (c) Miller, S. R.; Lear, E.; Gonzalez, J.; Slawin, A. M. Z.; Wright, P. A.; Guillou, N.; Férey, G. *Dalton Trans.* **2005**, 3319.

(3) (a) Ngo, H. L.; Lin, W. *J. Am. Chem. Soc.* **2002**, *124*, 14298. (b) Evans, O. R.; Ngo, H. L.; Lin, W. *J. Am. Chem. Soc.* **2001**, *123*, 10395. (c) Plutnar, J.; Rohovec, J.; Kotek, J.; Zak, Z.; Lukes, I. *Inorg. Chim. Acta* **2002**, *335*, 27.

(4) (a) Nash, K. L.; Rogers, R. D.; Ferraro, J.; Zhang, J. *Inorg. Chim. Acta* **1998**, *269*, 211. (b) Meervelt, L. V.; Martello, P.; Silvestre, J. P.; Rochdaoui, R.; Lee, M. R.; Dao, N. Q.; Walrand, C. G. *Z. Kristallogr.* **2002**, *217*, 27. (c) Shkolnikova, L. M.; Masyuk, A. A.; Polyanchuk, G. V.; Afonin, E. G.; Poznyak, A. L.; Zavodnik, V. E. *Koord. Khim.* **1989**, *15*, 1424.

(5) (a) Serre, C.; Stock, N.; Bein, T.; Ferey, G. *Inorg. Chem.* **2004**, *43*, 3159. (b) Cao, D.-K.; Li, Y.-Z.; Song, Y.; Zheng, L.-M. *Inorg. Chem.* **2005**, *44*, 3599.

(6) (a) Wang, R. C.; Zhang, Y. P.; Hu, H. L.; Frausto, R. R.; Clearfield, A. *Chem. Mater.* **1992**, *4*, 864. (b) Glowiak, T.; Huskowska, E.; Legendziewicz, J. *Polyhedron* **1991**, *10*, 175.

(7) Serpaggi, F.; Férey, G. *Inorg. Chem.* **1999**, *38*, 4741. (b) Avecilla, F.; Peters, J. A.; Geraldes, C. F. G. C. *Eur. J. Inorg. Chem.* **2003**, 4179.

(8) (a) Clearfield, A.; Sharma, C. V. K.; Zhang, B.-L. *Chem. Mater.* **2001**, *13*, 3099. (b) Bligh, S. W. A.; Choi, N.; Geraldes, C. F. G. C.; Knoke, S.; McPartlin, M.; Sanganee, M. J.; Woodroffe, T. M. *J. Chem. Soc., Dalton Trans.* **1997**, 4119. (c) Vojtisek, P.; Ciger, P.; Kotek, J.; Rudovsky, J.; Hermann, P.; Lukes, I. *Inorg. Chem.* **2005**, *44*, 5591.

(9) Silvestre, J. P.; Dao, N. Q.; Lee, M. R. *Phosphorus, Sulfur Silicon Relat. Elem.* **2001**, *176*, 173.

10.1021/ic0613255 CCC: $33.50

Table 1. Summary of Crystal Data and Structural Refinements for **1**−**6**

compound	**1**	**2**	**3**	**4**	**5**	**6**
empirical formula	$C_{60}H_{51}N_8O_{17.5}$-$P_2S_2La_2$	$C_{36}H_{40}N_4O_{20}$-$P_2S_2Nd_2$	$C_{36}H_{40}N_4O_{20}$-$P_2S_2Eu_2$	$C_{36}H_{40}N_4O_{20}$-$P_2S_2Er_2$	$C_{18}H_{57}N_4O_{30}$-P_5SLa_2	$C_{18}H_{57}N_4O_{30}$-P_5SNd_2
fw	1567.97	1263.26	1278.80	1309.30	1274.41	1285.07
space group	$P\bar{1}$	$P\bar{1}$	$P\bar{1}$	$P\bar{1}$	$I2/m$	$I2/m$
a/Å	14.5784(16)	12.2591(1)	12.2312(2)	12.174(3)	14.4085(1)	14.303(2)
b/Å	14.8856(13)	14.4243(2)	14.3800(3)	14.274(4)	18.9382(3)	18.7159(11)
c/Å	16.3402(17)	15.5038(1)	15.4760(2)	15.326(4)	17.0522(1)	17.0511(11)
α/deg	93.572(2)	112.633(1)	112.52	112.356(1)	90	90
β/deg	111.018(3)	107.991(1)	108.277(1)	108.382(2)	101.696(1)	102.118(2)
γ/deg	103.289(4)	98.390(1)	98.294(1)	98.416(2)	90	90
V/Å^3	3180.3(6)	2294.59(4)	2276.53(7)	2227.2(9)	4556.44(8)	4462.7(7)
Z	2	2	2	2	4	4
D_{calcd}/g cm^{-3}	1.637	1.828	1.865	1.952	1.858	1.913
μ/mm^{-1}	1.518	2.480	2.974	3.992	2.166	2.624
GOF on F^2	1.068	1.102	1.087	1.074	1.193	1.117
R1, wR2 [$I > 2\sigma(I)$][a]	0.0642 0.1584	0.0573, 0.1169	0.0490, 0.1017	0.0409, 0.0985	0.0672, 0.1244	0.0554, 0.1291
R1, wR2 (all data)[a]	0.0830, 0.1721	0.0693, 0.1253	0.0605, 0.1089	0.0504, 0.1077	0.0967, 0.1365	0.0630, 0.1352

[a] $R1 = \Sigma||F_o| - |F_c||/\Sigma|F_o|$. $wR2 = \{\Sigma w[(F_o)^2 - (F_c)^2]^2/\Sigma w[(F_o)^2]^2\}^{1/2}$.

been attached to the phosphonate ligand.[3−10] Results from our group indicate that introducing a second ligand such as 5-sulfoisophthalic acid or oxalic acid, whose lanthanide compounds have good solubility and very good crystallinity, into the lanthanide phosphonate system can also lead to novel luminescent lanthanide phosphonate hybrids.[11]

It is worth noting that a novel europium(III) phosphonate cage compound with a $\{Eu_9Na_6(L)_{16}\}^+$ (H_2L = 5′-methyl-2,2′-bipyridyl-6-phosphonic acid) cluster unit has a quantum yield as high as 32 ± 5% and its isostructural $\{Eu_{9-x}Yb_xNa_6(L)_{16}\}^+$ ($x = 4$ and 5) clusters display dual luminescence in the visible (Eu^{III}) and near-IR (Yb^{III}) ranges.[12] In addition to useful luminescent properties, lanthanide phosphonate cage compounds may also exhibit interesting magnetic properties.[15] Our current synthetic method for novel cluster lanthanide phosphonates is directly attaching a sulfonate group to a phosphonic acid and employing a suitable second ligand. The sulfonate group is strongly acidic; hence, it is anticipated that the introduction of the sulfonate group could greatly improve the solubility and crystallinity of lanthanide phosphonates. Also, a weak coordination sulfonate group attached on a phosphonic acid could be playing the role of controlling the dimension of the metal complexes. The introduction of an auxiliary ligand such as 1,10-phenanthroline (phen) reduces the coordination sites available for the phosphonate ligand and thereby facilitates the formation of cluster compounds. Furthermore, if a multidentate bridging ligand is used, the lanthanide sulfonate−phosphonate cluster units could be interconnected into 1D, layered, or porous 3D structures. In our current studies, we selected m-$HO_3SC_6H_4$-PO_3H_2 (H_3L^1) as the main ligand and phen or N,N'-piperazinebis(methylenephosphonic acid) (H_4L^2) as the auxiliary ligand. Applying such a synthetic technique to the transition-metal systems afforded three novel zinc(II) sulfonate−phosphonates with tetranuclear or hexanuclear cluster units.[16] Extension of such a method to the lanthanide systems resulted in six novel lanthanide(III) sulfonate−phosphonates based on tetranuclear clusters, namely, $[La_2(L^1)_2(phen)_4(H_2O)]\cdot 4.5H_2O$ (**1**), $[Ln_2(L^1)_2(phen)_2(H_2O)_5]\cdot 3H_2O$ (Ln = Nd, **2**; Eu, **3**; Er, **4**), and $[Ln_2(HL^1)(H_2L^2)_2(H_2O)_4]\cdot 8H_2O$ (Ln = La, **5**, Nd, **6**). Herein, we report their syntheses, crystal structures, and luminescent and magnetic properties.

Experimental Section

Materials and Instrumentations. m-Sulfophenylphosphonic acid (m-$HO_3SC_6H_4PO_3H_2$, H_3L^1) and N,N'-piperazinebis(methylenephosphonic acid) [$H_2O_3PCH_2N(C_2H_4)_2NCH_2PO_3H_2$, H_4L^2] were synthesized according to procedures previously reported.[10c,17] All other starting chemicals were obtained from commercial sources and used without further purification. Elemental analyses were performed on a German Elementary Vario EL III instrument. The Fourier transform IR (FT-IR) spectra were recorded on a Nicolet Magna 750 FT-IR spectrometer using KBr pellets in the range of 4000−400 cm^{-1}. Thermogravimetric analyses (TGA) were carried out on a NETZSCH STA 449C unit at a heating rate of 10 °C/min

---

(10) (a) Galdecka, E.; Galdecki, Z.; Gawryszewska, P.; Legendziewicz, J. *New J. Chem.* **2000**, *24*, 387. (b) Legendziewicz, J.; Gawryszewska, P.; Gałdecka, E.; Gałdecki, Z. *J. Alloys Compd.* **1998**, *275*, 356. (c) Groves, J. A.; Wright, P. A.; Lightfoot, P. *Inorg. Chem.* **2005**, *44*, 1736. (d) Rudovsky, J.; Cigler, P.; Kotek, J.; Hermann, P.; Vojtisek, P.; Lukes, I.; Peters, J. A.; Elst, L. V.; Muller, R. N. *Chem.*—*Eur. J.* **2005**, *11*, 2373. (e) Tang, S.-F.; Song, J.-L.; Mao, J.-G. *Eur. J. Inorg. Chem.* **2006**, 2011. (f) Bauer, S.; Bein, T.; Stock, N. *J. Solid State Chem.* **2006**, *179*, 145. (g) Yue, Q.; Yang, J.; Li, G.-H.; Li, G.-D.; Chen, J.-S. *Inorg. Chem.* **2006**, *45*, 4431.

(11) (a) Song, J.-L.; Lei, C.; Mao, J.-G. *Inorg. Chem.* **2004**, *43*, 5630. (b) Song, J.-L.; Mao, J.-G. *Chem.*—*Eur. J.* **2005**, *11*, 1417. (c) Ying, S.-M.; Mao, J.-G. *Cryst. Growth Des.* **2006**, 6, 964.

(12) Comby, S.; Scopelliti, R.; Imbert, D.; Charbonnière, L.; Ziessel, R.; Bünzli, J.-C. G. *Inorg. Chem.* **2006**, *45*, 3158.

(13) (a) Gan, X.-M.; Binyamin, I.; Rapko, B. M.; Fox, J.; Duesler, E. N.; Paine, R. T. *Inorg. Chem.* **2004**, *43*, 2443. (b) Gan, X.-M.; Rapko, B. M.; Fox, J.; Binyamin, I.; Pailloux, S.; Duesler, E. N.; Paine, R. T. *Inorg. Chem.* **2006**, *45*, 3741.

(14) (a) Richardson, F. S. *Chem. Rev.* **1982**, *82*, 541. (b) Horrocks, W. D.; Sudnik, D. R. *J. Am. Chem. Soc.* **1979**, *101*, 334. (c) Evans, C. H. Biochemistry of the Lanthanides. *Biochemistry of the Elements*; Plenum: New York, 1990; Vol. 8. (d) Legendziewicz, J. *J. Appl. Spectrosc.* **1995**, *62*, 189.

(15) (a) Ishikawa, N.; Sugita, M.; Wernsdorfer, W. *Angew. Chem., Int. Ed.* **2005**, *44*, 2931. (b) Xu, G.; Wang, Z. M.; He, Z.; Lu, Z.; Liao, C.-S.; Yan, C.-H. *Inorg. Chem.* **2002**, *41*, 6802. (c) Wang, R. Y.; Selby, H. D.; Liu, H.; Carducci, M. D.; Jin, T. Z.; Zheng, Z. P.; Anthis, J. W.; Staples, R. J. *Inorg. Chem.* **2002**, *41*, 278. (d) Wang, R. Y.; Liu, H.; Carducci, M. D.; Jin, T. Z.; Zheng, C.; Zheng, Z. P. *Inorg. Chem.* **2001**, *40*, 2743. (e) Wang, R. Y.; Zheng, Z. P.; Jin, T. Z.; Staples, R. J. *Angew. Chem., Int. Ed.* **1999**, *38*, 1813.

(16) Du, Z.-Y.; Xu, H.-B.; Mao, J.-G. *Inorg. Chem.* **2006**, *45*, 6424.

(17) (a) Montoneri, E. *Phosphorus, Sulfur Silicon Relat. Elem.* **1991**, *55*, 201. (b) Montoneri, E.; Gallazzi, M. C. *Dalton Trans.* **1989**, 1819.

Table 2. Selected Bond Lengths (Å) for Compounds **1**−**6**[a]

Compound **1**							
La1−O9#1	2.434(4)	La2−O7	2.356(4)	La1−O3#1	2.438(4)	La2−O2	2.339(4)
La1−O8	2.512(4)	La2−O1W	2.611(5)	La1−O1	2.582(4)	La2−O12#2	2.478(6)
La1−O9	2.688(4)	La2−N8	2.732(6)	La1−N4	2.772(6)	La2−N5	2.690(6)
La1−N1	2.778(5)	La2−N6	2.779(5)	La1−N2	2.778(5)	La2−N7	2.732(6)
La1−N3	2.802(5)						
Hydrogen Bonds							
O10···O8W#3	2.810(8)	O6W···O7W	2.80(3)	O1W···O8W#4	2.791(9)	O7W···O8W	2.84(2)
Compound **2**							
Nd1−O11#1	2.340(5)	Nd2−O13#1	2.306(5)	Nd1−O12	2.357(5)	Nd2−O23	2.361(5)
Nd1−O22#1	2.403(5)	Nd2−O5W	2.441(7)	Nd1−O21	2.422(5)	Nd2−O4W	2.509(6)
Nd1−O1W	2.577(6)	Nd2−O3W	2.519(6)	Nd1−N2	2.600(7)	Nd2−O2W	2.606(6)
Nd1−N1	2.620(7)	Nd2−N4	2.630(7)	Nd1−O22	2.676(5)	Nd2−N3	2.647(7)
Hydrogen Bonds							
O1W···O8W	2.65(2)	O6W···O7W	2.54(3)	O1W···O8W′	2.756(19)	O6W···O7W#2	2.65(3)
O4W···O9W	2.688(9)	O42···O4W#3	2.820(10)	O5W···O6W	2.59(2)	O43···O3W#3	2.713(9)
Compound **3**							
Eu1−O11#1	2.308(5)	Eu2−O13#1	2.260(5)	Eu1−O12	2.319(5)	Eu2−O23	2.326(5)
Eu1−O22#1	2.359(5)	Eu2−O5W	2.410(6)	Eu1−O21	2.370(5)	Eu2−O4W	2.459(6)
Eu1−O1W	2.547(5)	Eu2−O3W	2.488(6)	Eu1−N1	2.567(6)	Eu2−O2W	2.560(6)
Eu1−N2	2.572(6)	Eu2−N4	2.584(7)	Eu1−O22	2.667(5)	Eu2−N3	2.607(7)
Hydrogen Bonds							
O1W···O8W	2.66(2)	O6W···O7W#2	2.65(3)	O1W···O8W′	2.770(18)	O32···O3W#4	2.800(13)
O1W···O5W	2.830(8)	O42···O4W#3	2.824(10)	O4W···O9W	2.703(9)	O43···O3W#3	2.701(9)
O5W···O6W	2.605(19)	O43···O8W#5	2.85(2)	O6W···O7W	2.55(3)		
Compound **4**							
Er1−O11#1	2.253(4)	Er2−O13#1	2.205(4)	Er1−O12	2.262(4)	Er2−O23	2.268(4)
Er1−O22#1	2.289(4)	Er2−O5W	2.323(4)	Er1−O21	2.302(4)	Er2−O4W	2.388(5)
Er1−N2	2.492(5)	Er2−O3W	2.416(5)	Er1−O1W	2.497(4)	Er2−N4	2.520(5)
Er1−N1	2.499(5)	Er2−O2W	2.527(5)	Er1−O22	2.666(4)	Er2−N3	2.530(5)
Hydrogen Bonds							
O1W···O8W	2.643(15)	O6W···O7W	2.56(3)	O4W···O9W	2.694(7)	O32···O2W#4	2.719(18)
O5W···O6W	2.607(15)	O43···O3W#3	2.698(7)	O6W···O7W#2	2.55(2)		
Compound **5**							
La1−O23	2.425(6)	La2−O13#3	2.473(6)	La1−O23#1	2.425(6)	La2−O13	2.473(6)
La1−O32#2	2.506(6)	La2−O31#2	2.533(8)	La1−O32#3	2.506(6)	La2−O1W	2.587(9)
La1−O12	2.523(6)	La2−O2W	2.593(7)	La1−O12#1	2.523(6)	La2−O2W#3	2.593(7)
La1−O13	2.912(6)	La2−O3W	2.611(11)	La1−O13#1	2.912(6)	La2−O32	2.672(6)
		La2−O32#3	2.672(6)				
Hydrogen Bonds							
O11···O4W#4	2.740(14)	O3W···O5W#6	2.76(3)	O21···O8W#4	2.63(2)	O3W···O5W#4	2.76(3)
O21···O4W#3	2.755(16)	O8W···O10W#7	2.69(7)	O42···O9W#5	2.76(4)	O10W···O10W#1	2.51(10)
Compound **6**							
Nd1−O23	2.349(4)	Nd2−O13#2	2.403(4)	Nd1−O23#1	2.349(4)	Nd2−O13	2.403(4)
Nd1−O32#2	2.436(5)	Nd2−O31#3	2.456(6)	Nd1−O32#3	2.436(5)	Nd2−O3W	2.525(6)
Nd1−O12#1	2.455(4)	Nd2−O2W	2.526(5)	Nd1−O12	2.455(4)	Nd2−O2W#2	2.526(5)
Nd1−O13	2.933(4)	Nd2−O1W	2.545(7)	Nd1−O13#1	2.933(4)	Nd2−O32#2	2.649(4)
		Nd2−O32	2.649(4)				
Hydrogen Bonds							
O11···O4W#4	2.732(11)	O1W···O5W	2.77(2)	O21···O8W	2.59(4)	O1W···O5W#2	2.77(2)
O21···O4W#2	2.751(13)	O9W···O9W#5	2.76(9)	O43···O9W#5	2.53(4)	O7W···O9W#5	2.65(5)
O43···O9W	2.53(4)						

[a] Symmetry codes. For **1**: #1, $-x+1, -y, -z+1$; #2, $-x, -y, -z+1$; #3, $x, y, z+1$; #4, $-x, -y, -z$. For **2**−**4**: #1, $-x+2, -y+1, -z+1$; #2, $-x+1, -y, -z$; #3, $-x+1, -y+1, -z$; #4, $x, y+1, z+1$; #5, $x, y+1, z$. For **5**: #1, $-x-1, y, -z-1$; #2, $-x-1, -y+2, -z-1$; #3, $x, -y+2, z$; #4, $x-{}^1/_2, y+{}^1/_2, z-{}^1/_2$; #5, $-x+{}^1/_2, -y+{}^3/_2, -z-{}^1/_2$; #6, $x-{}^1/_2, -y+{}^3/_2, z-{}^1/_2$; #7, $x+{}^1/_2, y-{}^1/_2, z+{}^1/_2$. For **6**: #1, $-x-1, y, -z-1$; #2, $x, -y+1, z$; #3, $-x-1, -y+1, -z-1$; #4, $x-{}^1/_2, y+{}^1/_2, z-{}^1/_2$; #5, $-x, -y+1, -z-1$.

under an oxygen atmosphere. Photoluminescence analyses for compounds **2** and **3** were performed on an Edinburgh FLS920 and a Perkin-Elemer LS55 fluorescence spectrometer, respectively. Powder XRD patterns (Cu Kα) were collected on an XPERT-MPD $\theta-2\theta$ diffractometer. Magnetic susceptibility measurements for compounds **2**−**4** and **6** were performed with a PPMS-9T magnetometer in the temperature range of 2−300 K.

Preparation of $[La_2(L^1)_2(phen)_4(H_2O)]\cdot4.5H_2O$ (1). A mixture of $La(NO_3)_3\cdot6H_2O$ (0.4 mmol), H_3L^1 (0.4 mmol), and phen (0.45 mmol) in distilled water (10 mL), with the pH value adjusted to 5.0 by the addition of a 1 M NaOH solution, was sealed in an autoclave equipped with a Teflon liner (23 mL) and then heated at 150 °C for 4 days. Colorless brick-shaped crystals of **1** were collected in a ca. 38% yield based on lanthanum. Its purity has also been confirmed by powder XRD studies. Using $LaCl_3\cdot6H_2O$ instead of $La(NO_3)_3\cdot6H_2O$ as the lanthanum(III) source under the same react conditions gave a much lower yield (about 5.0%). Anal. Calcd for $C_{60}H_{51}O_{17.5}N_8La_2P_2S_2$ (M_r = 1567.97): C, 45.96; H, 3.28;

N, 7.15. Found: C, 46.19; H, 3.42; N, 7.12. IR data (KBr, cm^{-1}): 3436(s), 1625(m), 1591(m), 1516(m), 1424(m), 1178(s), 1115(vs), 1097(vs), 1030(s), 1000(s), 983(m), 845(m), 802(m), 731(m), 697(m), 619(m), 563(m).

Preparation of $[Ln_2(L^1)_2(phen)_2(H_2O)_5]\cdot 3H_2O$ (Ln = Nd, 2; Eu, 3; Er, 4). A mixture of $LnCl_3\cdot 6H_2O$ (0.4 mmol), H_3L^1 (0.4 mmol), and phen (0.4 mmol) in distilled water (10 mL), with the pH value adjusted to 4.0 by the addition of a 1 M NaOH solution, was sealed in an autoclave equipped with a Teflon liner (23 mL) and then heated at 150 °C for 4 days. Crystals of **2** (purple), **3** (colorless), and **4** (pink) were collected in about 56%, 61%, and 66% yield, respectively (based on the lanthanide). Their purities have also been confirmed by powder XRD studies. Anal. Calcd for $C_{36}H_{40}O_{20}N_4Nd_2P_2S_2$ (M_r = 1263.26): C, 34.23; H, 3.19; N, 4.44. Found: C, 34.31; H, 3.34; N, 4.23. Anal. Calcd for $C_{36}H_{40}O_{20}N_4Eu_2P_2S_2$ (M_r = 1278.80): C, 33.81; H, 3.15; N, 4.38. Found: C, 33.90; H, 3.47; N, 4.20. Anal. Calcd for $C_{36}H_{40}O_{20}N_4Er_2P_2S_2$ (M_r = 1309.30): C, 33.02; H, 3.08; N, 4.28. Found: C, 32.94; H, 3.12; N, 4.20. IR data (KBr, cm^{-1}) for **2**: 3348(s), 1658(m), 1520(m), 1426(m), 1180(s), 1127(vs), 1098(vs), 1032(s), 1000(s), 851(m), 802(m), 732(m), 701(m), 621(m), 566(m). IR data (KBr, cm^{-1}) for **3**: 3412(s), 1625(m), 1518(m), 1424(m), 1175(s), 1100(vs), 1060(s), 1031(vs), 1000(s), 846(m), 798(m), 731(m), 689(m), 619(m), 552(m). IR data (KBr, cm^{-1}) for **4**: 3419(s), 1626(m), 1521(m), 1426(m), 1179(s), 1130(vs), 1096(vs), 1031(s), 1002(s), 851(m), 803(m), 732(m), 701(m), 618(m), 567(m).

Preparation of $[Ln_2(HL^1)(H_2L^2)_2(H_2O)_4]\cdot 8H_2O$ (Ln = La, 5; Nd, 6). A mixture of $LnCl_3\cdot 6H_2O$ (0.45 mmol), H_3L^1 (0.45 mmol), and H_4L^2 (0.4 mmol) in distilled water (10 mL), with the pH value adjusted to 3.5 by the addition of a 1 M NaOH solution, was sealed in an autoclave equipped with a Teflon liner (23 mL) and then heated at 150 °C for 3 days. Crystals of **5** (colorless) and **6** (purple) were collected in about 69% and 33% yield, respectively (based on the lanthanide metal). Their purities have also been confirmed by powder XRD studies. Anal. Calcd for $C_{18}H_{57}O_{30}N_4La_2P_5S$ (M_r = 1274.41): C, 16.96; H, 4.51; N, 4.40. Found: C, 16.79; H, 4.26; N, 4.13. Anal. Calcd for $C_{18}H_{57}O_{30}N_4Nd_2P_5S$ (M_r = 1285.07): C, 16.82; H, 4.47; N, 4.36. Found: C, 16.63; H, 4.32; N, 4.11. IR (KBr, cm^{-1}) for **5**: 3435(s), 1642(w), 1457(w), 1140(vs), 1051(vs), 979(s), 961(m), 767(m), 617(w), 560(m), 467(w). IR (KBr, cm^{-1}) for **6**: 3412(s), 1638(w), 1457(w), 1108(vs), 1020(s), 998(s), 961(m), 768(m), 617(w), 558(m).

Single-Crystal Structure Determination. Data collections for compounds **2**, **3**, and **5** were performed on a Siemens Smart CCD diffractometer, whereas compounds **1**, **4**, and **6** were performed on a Mercury CCD diffractometer. Both diffractometers were equipped with graphite-monochromated Mo Kα radiation (λ = 0.710 73 Å). Intensity data were collected by the narrow-frame method at 293 K. The data sets were corrected for Lorentz and polarization factors as well as for absorption by the *SADABS* program[18a] or the multiscan method.[18b] All structures were solved by direct methods and refined by full-matrix least-squares fitting on F^2 by *SHELX-97*.[18c] All non-hydrogen atoms, except some disordered sulfonate oxygen atoms (O31 and O31′ in compound **2**; O33 in compound **3**; O31, O31′, O32, and O32′ in compounds **3** and **4**; O41, O42, and O43 in compounds **5** and **6**) and several lattice water molecules (O8W and O8W′ in compounds **3** and **4** as well as O10W in compounds **5** and **6**), were refined with anisotropic thermal parameters. The S1 atom in compounds **5** and **6** is also disordered with a S···S distance of 1.26(2) Å; hence, its occupancy factor is reduced to 50%. All hydrogen atoms were generated geometrically and refined isotropically. The hydrogen atoms for the water molecules are not included in the refinements. The disordered sulfonate oxygen atoms and lattice water molecules (see above) display two orientations with 50% occupancy for each site. Crystallographic data and structural refinements for compounds **1**−**6** are summarized in Table 1. Important bond lengths are listed in Table 2. More details about crystallographic studies are given in the Supporting Information.

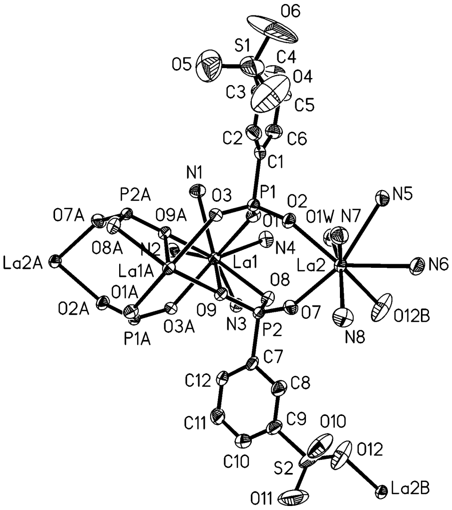

Figure 1. ORTEP representation of the selected unit of **1**. The thermal ellipsoids are drawn at 50% probability. Lattice water molecules and the carbon atoms of the phen ligands have been omitted for clarity. Symmetry codes for the generated atoms: a, $1 - x, -y, 1 - z$; b, $-x, -y, 1 - z$.

Results and Discussion

Compounds **1**−**6** represent the first members of lanthanide(III) complexes of sulfonate−phosphonate ligands. More interestingly, they display isolated, 1D, and 3D structures based on two types of tetranuclear lanthanide units. The dimension of the structure is controlled by mainly the lanthanide ionic size, the binding modes of the sulfonate−phosphonate ligand, and the second metal linker.

Structure of 1. There are two unique lanthanum(III) ions in the asymmetric unit of compound **1**. As shown in Figure 1, La1 is nine-coordinated by five phosphonate oxygen atoms from four L^1 anions and two bidentate-chelating phen ligands, whereas La2 is eight-coordinated by two phosphonate oxygen atoms from two L^1 anions, one sulfonate oxygen atom from another L^1 anion, and two bidentate-chelating phen ligands as well as an aqua ligand. The La−O [2.339(4)−2.688(4) Å] and La−N [2.690(6)−2.802(5) Å] distances are comparable to those reported for other lanthanum phosphonate−sulfonates.[11]

There are two crystallographically distinct L^1 ligands. The ligand containing P1 and S1 is tridentate, with each phosphonate oxygen connecting with a lanthanum(III) ion. The other L^1 anion containing P2 and S2 is pentadentate by using its three phosphonate oxygen atoms and one sulfonate oxygen. The phosphonate group is tetradentate and bridges with three lanthanum(III) ions; one phosphonate oxygen atom (O9) functions as a μ^2-metal linker. The sulfonate group is

---

(18) (a) Sheldrick, G. M. *Program SADABS*; Universität Göttingen: Göttingen, Germany, 1995. (b) *CrystalClear*, version 1.3.5; Rigaku Corp.: Woodlands, TX, 1999. (c) Sheldrick, G. M. *SHELX-96 Program for Crystal Structure Determination*; Bruker AXS Inc.: Madison, WI, 1996.

Scheme 1. Structural Relationships of the Six Cluster Compounds[a]

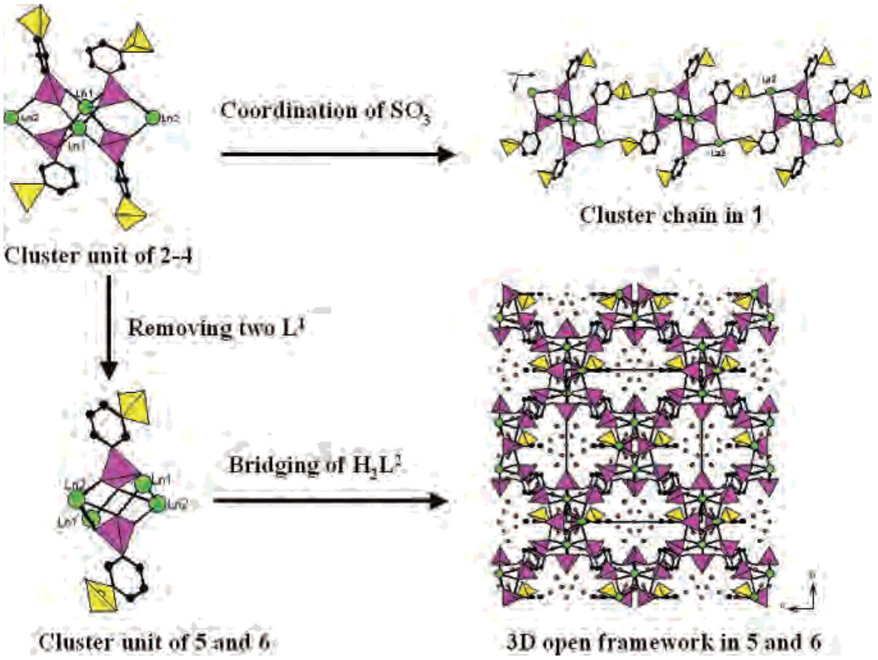

[a] The CPO_3 and CSO_3 groups are represented by pink and yellow, respectively.

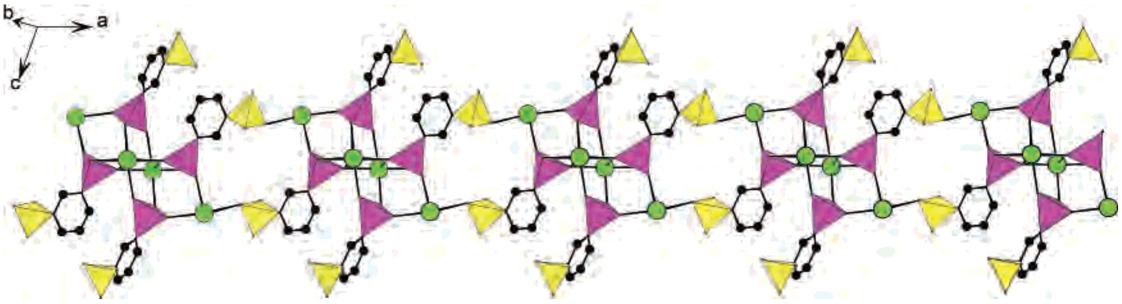

Figure 2. View of a 1D cluster chain along the *a* axis in compound **1**. The CPO_3 and CSO_3 tetrahedra are shaded in pink and yellow, respectively. The lanthanum and carbon atoms are drawn as green and black circles, respectively. The phen ligands and aqua ligands have been omitted for clarity.

unidentate. Two La1 and two La2 ions are interconnected by four phosphonate groups of four L^1 anions into a tetranuclear cluster unit (Scheme 1). The distances of La1···La2 edges are 5.809(1) and 5.887(1) Å, respectively, and the La1···La1 distance is 4.063(1) Å. Each phosphonate ligand caps on a Ln_3 triangle. Such tetranuclear cluster is connected to two neighboring ones through coordination of the sulfonate oxygen atoms, forming a 1D chain along the *a* axis (Figure 2). A number of hydrogen bonds are formed among the noncoordinated sulfonate oxygen atoms and the lattice water molecules (Table 2). There is also weak $\pi\cdots\pi$ interaction between the pyridyl rings of the phen ligands from neighboring chains. The distance from the center of the pyridyl ring formed by N5, C37, C38, C39, C40, and C48 to that of its symmetrically generated parallel one (symmetry code: $-x, -y, -z$) is 3.417 Å.

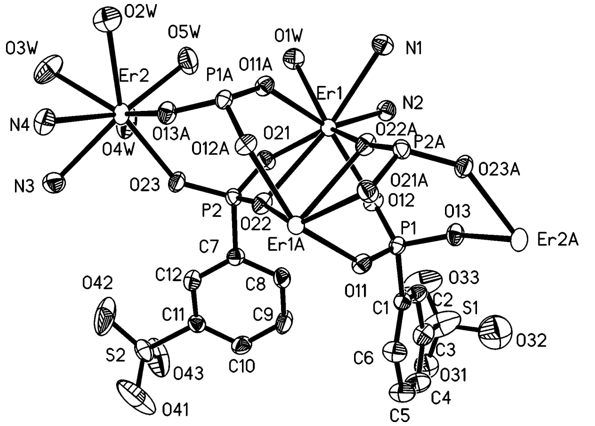

Figure 3. ORTEP representation of the selected unit in compound **4**. The thermal ellipsoids are drawn at 50% probability. Lattice water molecules and the carbon atoms of the phen ligands have been omitted for clarity. Only one orientation was shown for the disordered sulfonate oxygen atoms for the sake of clarity. Symmetry codes for the generated atoms: a, $2 - x$, $1 - y$, $1 - z$.

Structures of 2−4. When the lanthanum(III) ions were replaced by other lanthanide(III) ions, $[Ln_2(L^1)_2(phen)_2(H_2O)_5]\cdot 3H_2O$ (Ln = Nd, **2**; Eu, **3**; Er, **4**) complexes were isolated. Compounds **2**−**4** are isostructural; hence, only the structure of **4** will be discussed in detail as a representative. Compound **4** features a discrete tetranunuclear erbium(III) cluster. There are two unique erbium(III) ions (Figure 3): Er1 is eight-coordinated by five phosphonate oxygen atoms from four L^1 anions and a bidentate-chelating phen as well as an aqua ligand, whereas Er2 is eight-coordinated by two phosphonate oxygen atoms from two L^1 anions, a bidentate-

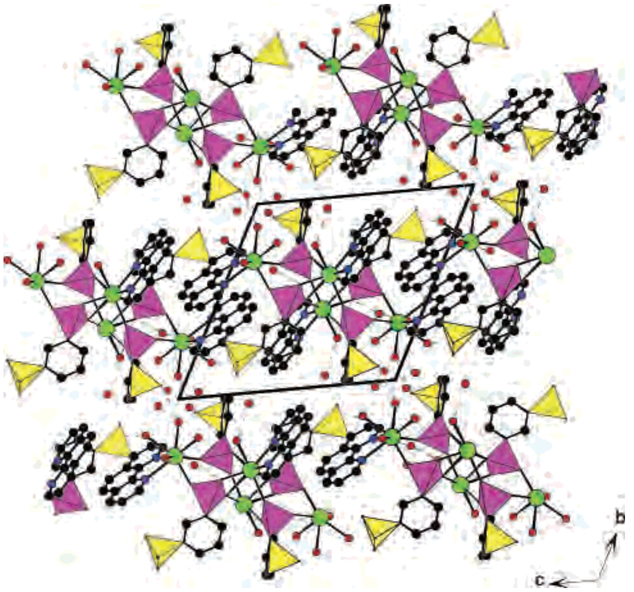

Figure 4. View of the structure of compound **4** down the *a* axis. The CPO_3 and CSO_3 groups are shaded in pink and yellow, respectively. The erbium, oxygen, and carbon atoms are drawn as green, red, and black circles, respectively.

chelating phen, and four aqua ligands. The Er−O [2.205(4)−2.666(4) Å] and Er−N [2.492(5)−2.530(5) Å] distances are slightly shorter than the La−O and La−N distances in compound **1** because of the “lanthanide contraction”.

The phosphonate groups of the L^1 ligands adopt the same coordination fashion as those in compound **1**. However, the sulfonate groups in compound **4** remain noncoordinated. Similar to those in compound **1**, two Er1 and two Er2 ions are bridged by four sulfonate−phosphonate ligands into a tetranuclear cluster (Scheme 1). It is noted that compound **1** contains one aqua ligand and four phen ligands per formula unit whereas compounds **2**−**4** each has five aqua ligands and two phen ligands per formula unit. It can be considered as that two of four phen ligands in compound **1** being replaced by four aqua ligands to form compounds **2**−**4**. Within the cluster, the four Er1···Er2 edges are 5.901(1) and 5.289(1) Å, respectively, and the Er1···Er1 distance is 3.811(1) Å. These discrete tetranuclear clusters in compound **4** are hydrogen-bonded into a 3D supramolecular network via hydrogen bonds among sulfonate oxygen atoms and lattice water molecules (Figure 4 and Table 2). There is also weak $\pi\cdots\pi$ interaction between the benzene rings of the phen ligands from neighboring cluster units in compound **4**. The distance from the center of the benzene ring formed by C26, C27, C28, C29, C33, and C34 to that of its symmetrically generated parallel one (symmetry code: $2 - x, 1 - y, -z$) is 3.408 Å.

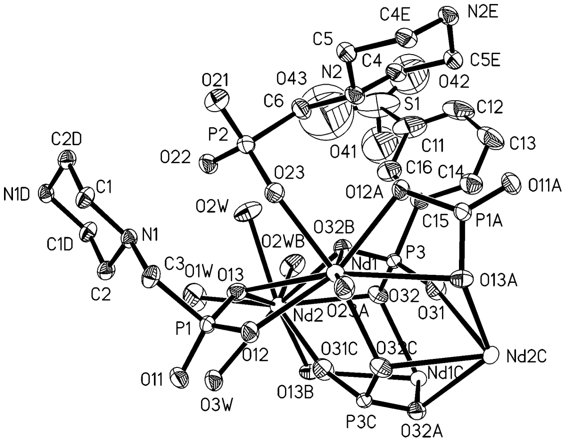

Figure 5. ORTEP representation of the selected unit of **6**. The thermal ellipsoids are drawn at 50% probability. The lattice water molecules have been omitted for clarity. Symmetry codes for the generated atoms: a, $-x - 1, y, -z - 1$; b, $x, -y + 1, z$; c, $-x - 1, -y + 1, -z - 1$; d, $x - {}^1/_2, y + {}^1/_2, z - {}^1/_2$; e, $-x, -y + 1, -z - 1$.

Structures of 5 and 6. Compounds **5** and **6** were isolated when H_4L^2 was applied as the second metal linker instead of phen, and the reaction medium is more acidic. Compounds **5** and **6** are isostructural; hence, only the structure of compound **6** will be discussed in detail. The structure of compound **6** features a 3D architecture based on different types of tetranuclear clusters. Among two unique neodymium(III) ions in compound **6**, Nd1 is eight-coordinated by six phosphonate oxygen atoms from four H_2L^2 anions and two phosphonate oxygen atoms from two HL^1 anions, whereas Nd2 is nine-coordinated by three phosphonate oxygen atoms from two HL^1 anion and two phosphonate oxygen atoms from two H_2L^2 anions as well as four aqua ligands (Figure 5). The Nd−O [2.349(4)−2.933(4) Å] distances are comparable to those in compound **2** and other neodymium(III) phosphonates previously reported.[1,11]

Different from those in compounds **1**−**4**, the phosphonate group of the HL^1 ligand in compound **6** is pentadentate, two phosphonate oxygen atoms act as μ^2-bridging ligand, whereas the third oxygen atom is monodentate. The sulfonate group of the HL^1 ligand is severely disordered and remains noncoordinated. Each HL^1 anion connects with four neodymium(III) ions (Chart 1a). The two H_2L^2 anions adopt two different coordination modes. The one containing P1 is tetradentate and bridges with four neodymium(III) ions from two cluster units (Chart 1). The one containing P2 is bidentate and connects with two neodymium(III) ions from two cluster units. The interconnection of four neodymium(III) ions by two bridging HL^1 ligands resulted in a novel tetranuclear cluster unit. The four neodymium(III) ions form a slightly distorted square with the two phosphonate groups of the HL^1 ligands capped above and below the square. Each Nd1···Nd2 edge is further bridged by a phosphonate group of a H_2L^2 anion. The Nd1···Nd2 edges of 4.181(1) Å are significantly shorter than those in compounds **1**−**4**. Such clusters are further cross-linked by bridging H_2L^2 anions into a 3D open framework with larger tunnels along the *a* axis. Each cluster is bridged to six neighbors. The size of the tunnel is estimated to be 6.2 × 7.6 Å^2 based on structural data. The lattice water molecules are located in the above tunnels (Figure 6). A number of hydrogen bonds are formed among the noncoordinated sulfonate oxygen atoms, the aqua ligands, and the lattice water molecules, which further increases the stability of the structure (Table 2). The total solvent-accessible space is about 23.3% of the cell volume

Chart 1 Coordination Modes of HL^1 and H_2L^2 Anions in Compound **6**

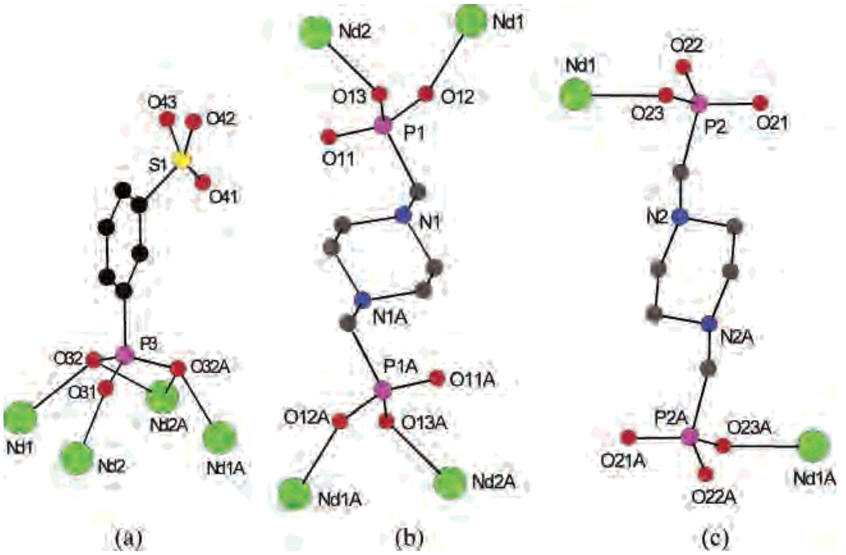

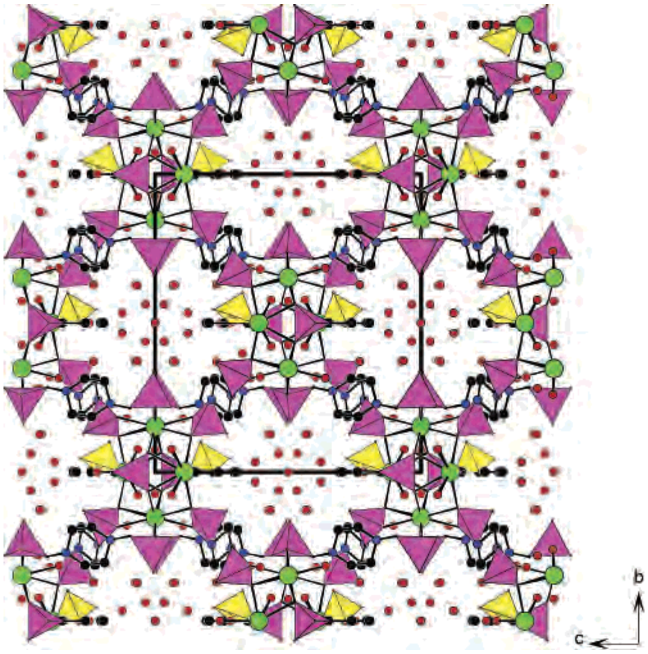

Figure 6. View of the structure of **6** along the *a* axis. The phosphonate and sulfonate groups are shaded in pink and yellow, respectively. Only one type of two orientations of the sulfonate group is shown. The neodymium, nitrogen, oxygen, and carbon atoms are drawn as green, blue, red, and black circles, respectively.

according to our calculations.[19] For compound **5**, this value is about 23.8%.

It is found that the open framework of compound **5** remains intact after heating at 150 °C for 4 h based on powder XRD studies (see the Supporting Information).

Luminescent Properties. The solid-state luminescent spectra of compounds **2**−**4** and **6** were investigated at room temperature. Compounds **4** and **6** did not show characteristic emission bands of the erbium(III) or neodymium(III) ion in the near-IR region, which may be ascribed to the "quenching effect" of the aqua ligands and lattice water molecules. Under excitation of 335 nm, compound **2** displays the characteristic emission bands for the neodymium(III) ion: a middle emission band at 890 nm with a shoulder band at 879 nm ($^4F_{3/2} \rightarrow {}^4I_{9/2}$), a strong emission band at 1061 nm with a shoulder band at 1072 nm ($^4F_{3/2} \rightarrow {}^4I_{11/2}$), and a weak band at 1335 nm ($^4F_{3/2} \rightarrow {}^4I_{13/2}$) in the near-IR region (Figure 7a).[11] The existence of shoulder bands further confirms that there are two unique neodymium(III) ions in compound **2**. Compound **3** exhibits three strong characteristic emission bands for the europium(III) ion in the visible region under excitation at 337 nm (Figure 7b). These emission bands are 535 nm ($^5D_0 \rightarrow {}^7F_0$), 591 nm ($^5D_0 \rightarrow {}^7F_1$), 615 nm ($^5D_0 \rightarrow {}^7F_2$), and 685 nm ($^5D_0 \rightarrow {}^7F_4$).[11] The Eu ($^5D_0$) lifetime of compound **3** for $\lambda_{ex,em} = 337$ and 614 nm is measured to be 0.29 ms.

Magnetic Property Studies. The temperature-dependent magnetic susceptibility data of compounds **2**−**4** and **6** have been measured for polycrystalline samples in the temperature range of 2−300 K. Plots of χ_M and $1/\chi_M$ vs T for compounds **2**−**4** and **6** are shown in Figure 8. Compounds **2**, **4**, and **6** obey the Curie−Weiss law above 50, 25, and 100 K, respectively, whereas compound **3** does not obey the law in most of temperature region. At 300 K, the effective magnetic moments (μ_{eff}) are measured to be 4.88, 4.61, 13.30, and 4.74 μ_B respectively for compounds **2**−**4** and **6**, which are slightly smaller than the theoretical values for the two isolated magnetic centers per formula unit (5.20, 4.81, 13.58, and 5.20 μ_B, respectively), which are calculated according to the Van Vleck formula, which includes the contributions from the spin−orbital interactions.[20] Upon cooling, the μ_{eff} values are decreased and reach 3.01, 0.455, 9.62, and 2.67 μ_B, respectively, for the four compounds, which indicates that there exist significant antiferromagnetic interactions between magnetic centers in all four compounds. It is expected that such antiferromagnetic interactions occur mainly between magnetic centers within the cluster units. Magnetic interactions between cluster units are expected to be weak because

---

(19) Spek, A. L. *Platon: A Multi-purpose Crystallographic Tool*; Utrecht University: Utrecht, The Netherlands, 2001.

(20) Van Vleck, J. H. *The Theory of Electric and Magnetic Susceptibilities*; Oxford University: Oxford, U.K., 1932; pp 226−261.

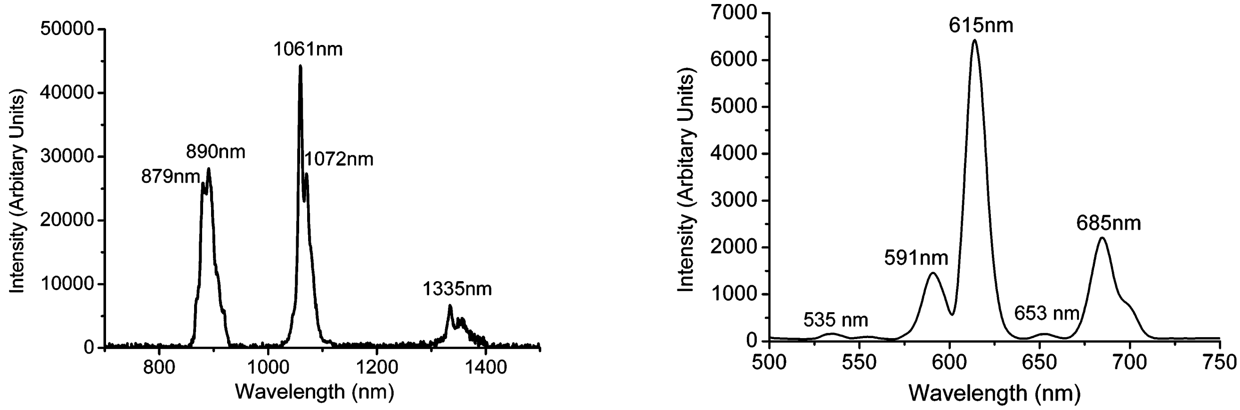

(a) (b)

Figure 7. Solid-state emission spectra of compounds **2** (a) and **3** (b).

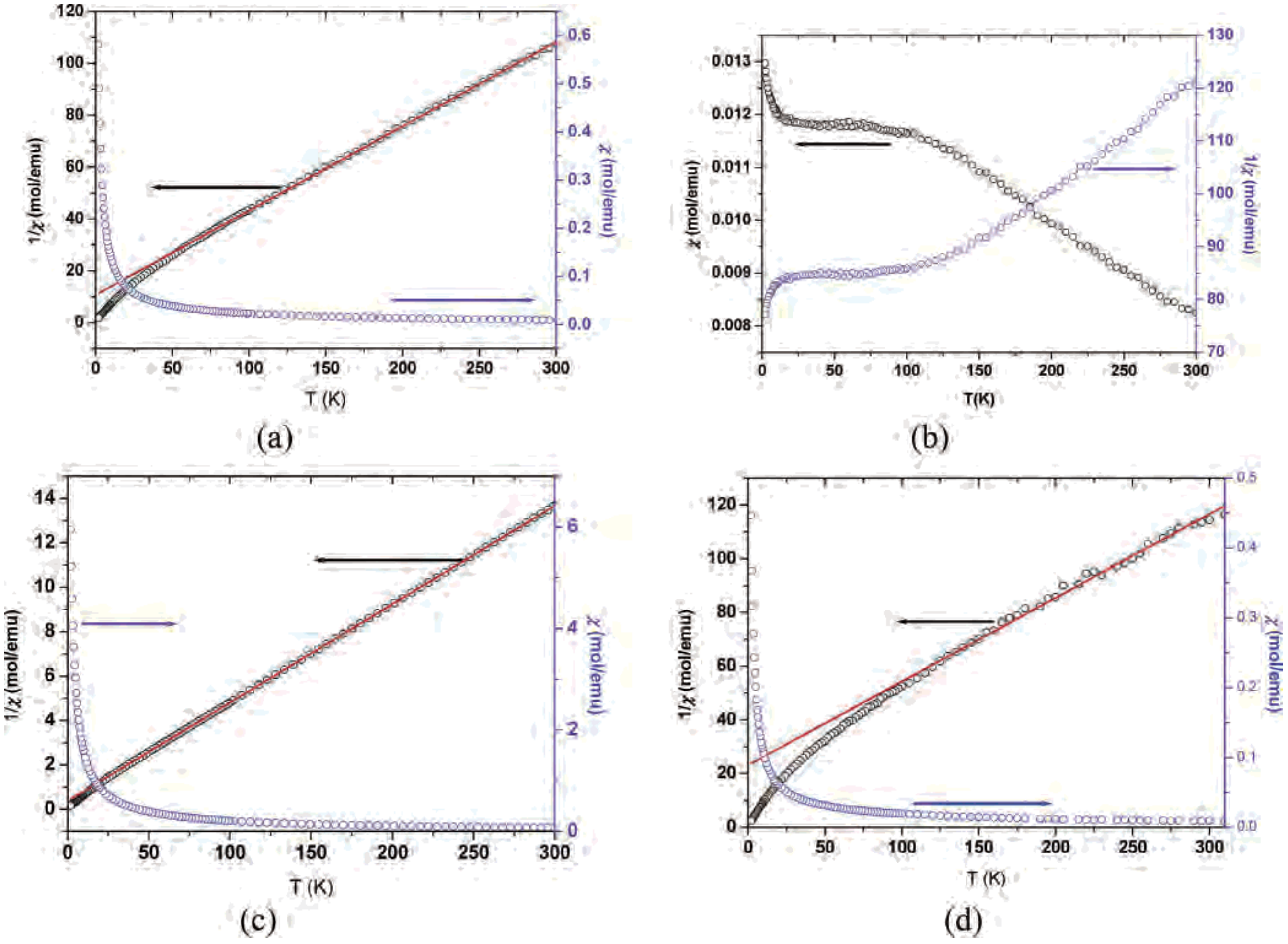

Figure 8. Plots of the temperature dependence of χ_M (blue points) and $1/\chi_M$ (black points) for compounds **2** (a), **3** (b), **4** (c), and **6** (d). The red lines show the best fit to the Curie−Weiss law.

these cluster units are well separated (>10 Å). Linear fitting of $1/\chi_M$ with T according to the Curie−Weiss law gave Weiss constants of −36(1), −8.5(2), and −94(3) K, respectively, for compounds **2**, **4**, and **6**. It is noted that the magnetic behavior of compound **3** is different from those of compounds **2**, **4**, and **6**. Its molar susceptibility increases almost linearly from 100 to 300 K, and then it changes very slowly until around 20 K, below which a sharp increase is observed. Such magnetic behavior has been reported in the europium(III) complex of 1,3,5-benzenetricarboxylic acid.[21] The much more negative value of the Weiss constant for compound **6** compared with that of compound **2** is due to much shorter Nd···Nd distances of the cluster in compound **6**. It should be pointed out that, because of the complexity of the structures as well as the lack of suitable models, more

---

(21) (a) Yang, J.; Yue, Q.; Li, G.-D.; Cao, J.-J.; Li, G.-H.; Chen, J.-S. *Inorg. Chem.* **2006**, *45*, 2857.

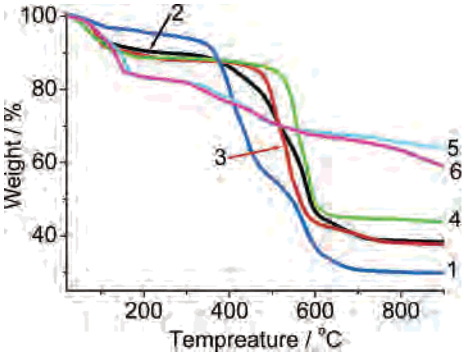

Figure 9. TGA curves for compounds **1**−**6**.

detailed calculations of the magnetic interactions for compounds **2**−**4** and **6** seem to be difficult.

TGA Studies. TGA curves of compound **1** exhibit two main steps of weight losses (Figure 9). The first step started at 40 °C and completed at 320 °C, which corresponds to the release of aqua ligands and lattice water molecules. The observed weight loss of 6.0% is close to the calculated value (6.3%). The second started at 320 °C and completed at 714 °C, during which the organic groups were combusted. The final residual is $LaPO_4$ based on powder XRD studies. The total observed weight loss of 70.1% is close to the calculated value (70.2%). TGA curves of compounds **2**−**4** are similar and exhibit two main steps of weight losses. The first step corresponds to the release of aqua ligands and lattice water molecules. The second corresponds the combustion of the organic groups. The final residuals are $LnPO_4$. The total observed weight losses of 61.6% (for **2**), 62.3% (for **3**), and 57.3% (for **4**) are close to the calculated values (62.1%, 61.4%, and 60.0% for compounds **2**−**4**, respectively). TGA curves of compounds **5** and **6** are similar, and each exhibits two main steps of weight loss. The first step (40−176 °C for compound **5** and 40−160 °C for compound **6**) corresponds to the release of 12 water molecules per formula unit. The observed weight losses of 16.1% and 16.0% are close to the calculated values (16.9% and 16.8%). The second step (about 300−500 °C) corresponds to the partial decomposition of the two types of organic ligands. The third step (about 500−900 °C) overlaps with the second one, during which the compounds are further decomposed. The total observed weight losses of 36.5% and 40.8% respectively for compounds **5** and **6** and the final residuals are not characterized. From the slopes of the TGA curves, we expect that the decomposing process is not complete at 900 °C.

Conclusion

In summary, six novel lanthanide(III) sulfonate−phosphonates have been synthesized by hydrothermal reactions and structurally characterized. Their structures are based on tetranuclear lanthanide sulfonate−phosphonate clusters. In compounds **2**−**4**, the cluster units are isolated, and in compound **1**, these clusters are interconnected into a 1D chain through the coordination of the sulfonate groups. The size of the cation plays an important role because a larger cation usually requires a higher coordination number. The use of phen also helps the formation of low-dimensional clusters because of its bidentate-chelating nature. When the second metal linker acts as the bridge between two cluster units, 3D cluster compounds can be formed, as in compounds **5** and **6** as well as the zinc cluster compound we reported previously.[16] This demonstrates that by choosing a sulfonate−phosphonate ligand as the main ligand and a suitable second ligand as well as a desirable metal ion, we could design metal sulfonate−phosphonate cluster compounds with controlled dimensions. Further research works will be devoted to the design of other types of sulfonate−phosphonic acids and studies on the crystal structures and physical properties of their metal complexes.

Acknowledgment. This work is supported by the National Natural Science Foundation of China (Grants 20371047, 20521101, and 20573113) and NSF of Fujian Province (Grant E0420003).

Supporting Information Available: X-ray crystallographic files in CIF format and XRD patterns for the six compounds. This material is available free of charge via the Internet at http://pubs.acs.org.

IC0613255